

Article

# Development of Circularly Polarized Luminescence (CPL) Peptides Containing Pyrenylalanines and 2-Aminoisobutyric Acid

Yuki Mimura, Yuki Motomura, Mizuki Kitamatsu \*  and Yoshitane Imai \* 

Department of Applied Chemistry, Faculty of Science and Engineering, Kindai University, 3-4-1 Kowakae, Higashi-Osaka, Osaka 577-8502, Japan; appletea0424@gmail.com (Y.M.); motomurayuki0818@gmail.com (Y.M.)

\* Correspondence: kitamatu@apch.kindai.ac.jp (M.K.); y-imai@apch.kindai.ac.jp (Y.I.)

Received: 31 October 2020; Accepted: 25 November 2020; Published: 27 November 2020



**Abstract:** Chiral organic and organometallic luminophores that possess circularly polarized luminescence (CPL) properties in the near-ultraviolet to near-infrared region have several useful applications. However, the CPL properties are subject to inherent factors of the compounds; to date, studies on the CPL properties influenced by amino acids and peptides are scarce. Consequently, we developed peptide-pyrene organic luminophores exhibiting various CPL properties. It is conceivable that the peptide-pyrene organic luminophores can be obtained as aggregates when dissolved in a solution. It is also possible that the formation of aggregates makes it difficult to accurately examine the CPL of the peptide in the solution. This study showed that the introduction of sterically hindered 2-aminoisobutyric acid (Aib) units into the peptide backbone inhibits aggregate formation. The resulting luminophores exhibit CPL properties owing to the presence of pyrene units. The results of this study can form a basis for the design of future materials that use peptide-pyrene organic luminophores.

**Keywords:** chiral; circularly polarized luminescence (CPL); pyrene; peptide

## 1. Introduction

It has been recently proposed that chiral organic and organometallic luminophores with circularly polarized luminescence (CPL) properties in the near-ultraviolet to near-infrared region can be employed in a variety of useful applications, such as 3D displays and photonic devices (e.g., organic LEDs) [1–11]. However, very few studies have investigated the effects of amino acids and peptides on the CPL properties. We previously investigated peptide-pyrene organic luminophores exhibiting CPL properties where no aggregate formation took place between pyrene units and found that chiral oligopeptides with multiple pyrene units exhibit a strong CPL signal from the excimers. However, it is possible that the pyrenes may form aggregates. In fact, agglomerates of pyrene have been observed when the number of pyrene moieties is increased. Therefore, it is difficult to purify a peptide containing five or more pyrene moieties due to such aggregate formation. To address this issue, we investigate various methods to prevent the formation of aggregates. In this work, we introduce a sterically hindered 2-aminoisobutyric acid (Aib) spacer between the pendant pyrenyl groups to inhibit aggregate formation. In addition, we synthesize an optically active Aib peptide-pyrene luminophore that increases the number of pyrene moieties incorporated into a single peptide (Figure 1a): (1) **D-Aib1**, (2) **D-Aib2**, (3) **D-Aib3**, (4) **D-Aib4**, (5) **D-Aib5**, and their corresponding *L*-isomers (**L-Aib1–L-Aib5**). The CPL properties of these peptides in a chloroform (CHCl<sub>3</sub>) solution are then investigated. Furthermore, we compare the glycine-containing Gly peptide, which contains more flexible units than the Aib

(Figure 1b) with previously reported peptide-pyrene luminophores containing two to four pyrene moieties (Figure 1c) [12].

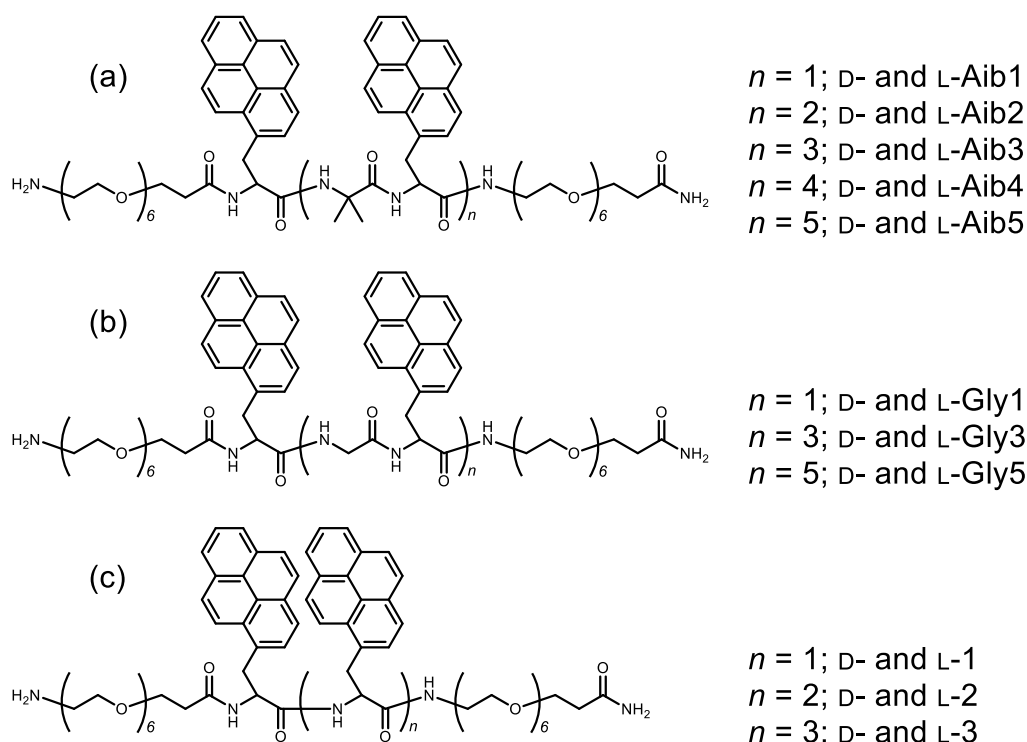


**Figure 1.** (a) Chiral 2-aminoisobutyric acid (Aib)-pyrenyl oligopeptide luminophores **D-Aib1–D-Aib5** and **L-Aib1–L-Aib5**. (b) Chiral Gly-pyrenyl oligopeptide luminophores **D-Gly1**, **D-Gly3**, **D-Gly5**, and their L-isomers. (c) Chiral pyrenyl oligopeptide luminophores **D-1–D-3** and **L-1–L-3**.

## 2. Materials and Methods

### 2.1. Synthesis of Chiral Aib-Pyrenyl Oligopeptides

The chiral Aib-pyrenyl oligopeptides were prepared by using previously reported conventional 9-fluorenylmethoxycarbonyl group (Fmoc)-based solid-phase peptide synthesis [12]. The peptides were synthesized using L-pyrenyl alanine (L-Ala(Pyr); Fmoc-Ala(1-Pyn)-OH), D-pyrenyl alanine (D-Ala(Pyr): Fmoc-D-Ala(1-Pyn)-OH), Aib (Fmoc-NH-C(CH<sub>3</sub>)<sub>2</sub>-OH), and an amino acid consisting of six ethylene glycol units (Sp6: Fmoc-NH-PEG<sub>6</sub>-COOH) as monomer units. Fmoc-Ala(1-Pyn)-OH, Fmoc-D-Ala(1-Pyn)-OH, and Fmoc-NH-C(CH<sub>3</sub>)<sub>2</sub>-OH were purchased from Watanabe Chemicals (Hiroshima, Japan). Fmoc-NH-PEG<sub>6</sub>-COOH was purchased from Merck (Darmstadt, Germany). The Sp6 linker was used for improving the affinity of the peptides against various solvents. The synthesized peptides exhibited the following sequences: H-Sp6-D-Ala(Pyr)-Aib-D-Ala(Pyr)-Sp6-NH<sub>2</sub> (**D-Aib1**), H-Sp6-(D-Ala(Pyr)-Aib)<sub>2</sub>-D-Ala(Pyr)-Sp6-NH<sub>2</sub> (**D-Aib2**), H-Sp6-(D-Ala(Pyr)-Aib)<sub>3</sub>-D-Ala(Pyr)-Sp6-NH<sub>2</sub> (**D-Aib3**), H-Sp6-(D-Ala(Pyr)-Aib)<sub>4</sub>-D-Ala(Pyr)-Sp6-NH<sub>2</sub> (**D-Aib4**), H-Sp6-(D-Ala(Pyr)-Aib)<sub>5</sub>-D-Ala(Pyr)-Sp6-NH<sub>2</sub> (**D-Aib5**), H-Sp6-L-Ala(Pyr)-Aib-L-Ala(Pyr)-Sp6-NH<sub>2</sub> (**L-Aib1**), H-Sp6-(L-Ala(Pyr)-Aib)<sub>2</sub>-L-Ala(Pyr)-Sp6-NH<sub>2</sub> (**L-Aib2**), H-Sp6-(L-Ala(Pyr)-Aib)<sub>3</sub>-L-Ala(Pyr)-Sp6-NH<sub>2</sub> (**L-Aib3**), H-Sp6-(L-Ala(Pyr)-Aib)<sub>4</sub>-L-Ala(Pyr)-Sp6-NH<sub>2</sub> (**L-Aib4**), and H-Sp6-(L-Ala(Pyr)-Aib)<sub>5</sub>-L-Ala(Pyr)-Sp6-NH<sub>2</sub> (**L-Aib5**).

These peptides were prepared on an Fmoc-NH-super acid-labile poly(ethylene glycol (SAL PEG)) resin (Watanabe Chemicals; 14 μmol Fmoc on a resin surface). The deprotection of Fmoc was carried out using 20% piperidine in N,N'-dimethylformamide (DMF) for 7 min. After washing the peptides six times with DMF, each Fmoc-derivatized amino acid was coupled with O-(1H-benzotriazol-1-yl)-N,N,N',N'-tetramethyluronium hexafluorophosphate (HBTU)/N-methylmorpholine (NMM) in DMF for 50 min. Deprotection and coupling processes were carried out at room temperature without a capping process. The peptides were cleaved from

the resin by treatment with 95.0:2.5:2.5 (v/v) trifluoroacetic acid (TFA)/water/triisopropylsilane (TIS) for 90 min at room temperature. Crude peptides were purified by reverse-phase high-performance liquid chromatography (RP-HPLC) on a C18 preparative column (Cadenza 5CD-C18; Imtakt, Kyoto, Japan) using a linear gradient from 35% to 100% (**D-Aib1** and **L-Aib1**), from 45% to 100% (**D-Aib2** and **L-Aib2**), from 50% to 100% (**D-Aib3** and **L-Aib3**), from 60% to 100% (**D-Aib4** and **L-Aib4**), and from 85% to 100% (**D-Aib5** and **L-Aib5**) of B solvent (acetonitrile; A solvent was 0.1% TFA ap.) over 30 min at a flow rate of 10.0 mL/min and monitored at 340 nm. The final product was identified using a C18 analytical column (Cadenza CD-C18 (CD003); Imtakt, Kyoto, Japan) and matrix-assisted laser desorption/ionization-time-of-flight (MALDI-TOF) mass spectrometry (Shimadzu AXIMA Confidence) (see Supporting Information: Figures S1–S20). The yields of the peptides were 49% (**D-Aib1**), 36% (**D-Aib2**), 10% (**D-Aib3**), 20% (**D-Aib4**), 9% (**D-Aib5**), 36% (**L-Aib1**), 44% (**L-Aib2**), 9% (**L-Aib3**), 21% (**L-Aib4**), and 6% (**L-Aib5**). **D-Gly1**, **D-Gly3**, **D-Gly5**, **L-Gly1**, **L-Gly3**, **L-Gly5**, **D-1**, **D-2**, **D-3**, **L-1**, **L-2**, and **L-3** were synthesized using previously reported methods [13].

## 2.2. Measurement of Circularly Polarized Luminescence (CPL) and Photoluminescence (PL) Spectra

Absolute PL quantum yields in CHCl<sub>3</sub> solutions and ethanol solution were obtained using an absolute PL quantum yield measurement system (Hamamatsu Photonics C9920-02, Hamamatsu Photonics, Hamamatsu, Japan) under air at room temperature. Luminophores **1–3** and **Aib1–Aib5**, each at a concentration of  $1.0 \times 10^{-4}$  M, in CHCl<sub>3</sub> solutions, were excited at 340 and 300 nm. Luminophores **1–3** and **Aib1–Aib5**, each at a concentration of  $1.0 \times 10^{-4}$  M, in ethanol solutions were excited at 300 nm, respectively. The pass length was 10 mm.

CPL and PL spectra in CHCl<sub>3</sub> solutions and ethanol solution were measured using a CPL-300 spectrofluoropolarimeter (JASCO, Tokyo, Japan) at room temperature. The instrument uses a scattering angle of 0° from the excitation of unpolarized, monochromated incident light with a bandwidth of 10 nm and a bandwidth for emission of 10 nm. The scanning speed was 50 nm min<sup>-1</sup> and the time constant of PMT (photomultiplier tube) was 8 s. The CPL and PL spectra were smoothed by two accumulations without any numerical smoothing. Luminophores **1–3** at a concentration of  $1.0 \times 10^{-4}$  M in CHCl<sub>3</sub> solutions were excited at 340 nm. Under the same conditions (i.e., concentration of  $1.0 \times 10^{-4}$  M in CHCl<sub>3</sub> solutions), luminophores **Aib1–Aib5** and Gly peptides (**Gly1**, **Gly3**, and **Gly5**) were excited at 300 nm. The pass length was 1 mm in CHCl<sub>3</sub>. Luminophores **1–3**, **Aib1–Aib5**, and Gly peptides (**Gly1**, **Gly3**, and **Gly5**) were excited at 300 nm. The pass length was 2 mm (**1–3** and **Aib1–Aib5**) and 1 mm (**Gly1**, **Gly3**, and **Gly5**) in ethanol solution.

## 2.3. Measurement of Circular Dichroism (CD) and UV–Vis Absorption Spectra

CD and UV–Vis absorption spectra of **Aib1–Aib5** and **1–3** and Gly peptides (**Gly1**, **Gly3**, and **Gly5**) in CHCl<sub>3</sub> solutions and ethanol solution ( $1.0 \times 10^{-4}$  M) were measured using a JASCO J-820 spectropolarimeter at room temperature. The pass length was 1 mm in CHCl<sub>3</sub>. In ethanol, the pass length was 2 mm (**1–3** and **Aib1–Aib5**) and 1 mm (**Gly1**, **Gly3**, and **Gly5**).

## 3. Results and Discussion

### 3.1. Measurement of Aib1–Aib5 Circularly Polarized Luminescence (CPL) and Photoluminescence (PL) Spectra and Circular Dichroism (CD) and UV–Vis Absorption Spectra in CHCl<sub>3</sub> Solution

The unpolarized photoluminescence (PL) and CPL spectra of **D-Aib1–D-Aib5** and **L-isomer (L-Aib1–L-Aib5)** in CHCl<sub>3</sub> solution ( $1.0 \times 10^{-4}$  M) were measured to investigate the effect of number of pyrenes and Aib units. Although the common problem in organic luminophores is aggregation-induced quenching [14], **D-Aib1–D-Aib5** emitted PL from the fluorescent pyrene units in the CHCl<sub>3</sub> solution (Figure 2a–e) for **D-Aib1–D-Aib5**, indicated by the red lines in the lower panels. As anticipated, **D-Aib1–D-Aib5** emitted both the monomer and excimer PLs. The excimer PL increased in the order **D-Aib1** < **D-Aib2** < **D-Aib3** < **D-Aib4** < **D-Aib5**. The maximum wavelengths of monomer PL emissions

( $\lambda_{em}$ ) for **D-Aib1–D-Aib5** were 379, 395.5, 395.5, 395.5, and 395.5 nm (L-isomer: 379, 395.5, 395.5, 395.5, and 395.5 nm, respectively). On the other hand, the corresponding excimer PL emissions ( $\lambda_{em}$ ) were 473.5, 460.5, 449, and 451.5 nm, respectively (L-isomer: 474.5, 453.5, 448, and 451.5 nm, respectively). Although the monomer-to-excimer emission intensity ratio increased in the order **Aib1** < **Aib2** < **Aib3** < **Aib4** < **Aib5**, no clear differences between the  $\lambda_{em}$  values of the monomer and excimer PLs were observed. The corresponding PL quantum yields ( $\Phi_F$ ) for **Aib1–Aib5** were 0.11, 0.12, 0.12, 0.14, and 0.17, respectively. The relatively low  $\Phi_F$  values for **Aib1–Aib5** result from the flexibility of the peptide backbone in the oligopeptide luminophores.

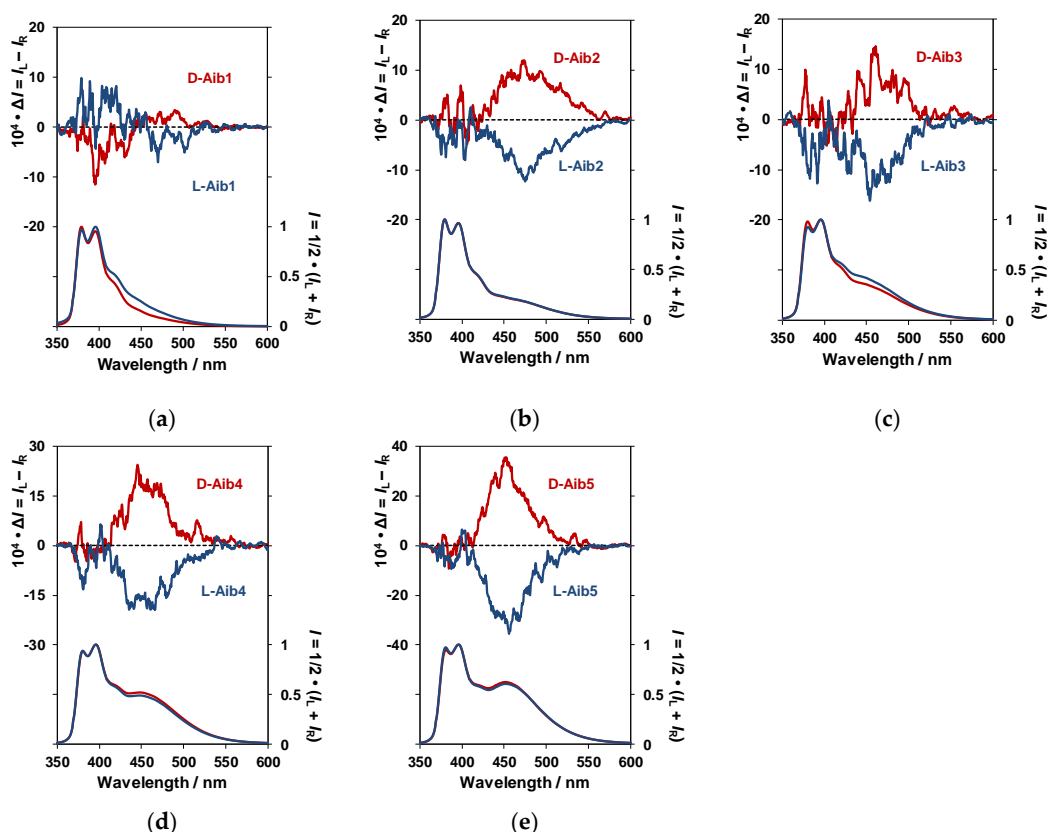


**Figure 2.** Circularly polarized luminescence (CPL) (upper panel) and photoluminescence (PL) (lower panel) spectra of (a) **D-Aib1/L-Aib1**; (b) **D-Aib2/L-Aib2**; (c) **D-Aib3/L-Aib3**; (d) **D-Aib4/L-Aib4**; and (e) **D-Aib5/L-Aib5** in  $\text{CHCl}_3$  ( $1.0 \times 10^{-4}$  M). D-isomer and L-isomer spectra are shown in red and blue, respectively. Path length = 1 mm.

The CPL intensity was quantitatively evaluated using the formula,  $g_{\text{CPL}} = \Delta I/I = (I_L - I_R)/(I_L + I_R)/2$ , in which  $I_L$  and  $I_R$  are the output signal intensities for left- and right-handed circularly polarized light, respectively, under unpolarized photoexcitation conditions. For **Aib1**, no clear CPL spectra were observed (upper panel of Figure 2a, indicated by the red and blue lines). In addition, the CPL spectra of **Aib2–Aib5** in  $\text{CHCl}_3$  were quite different from that of **Aib1**, as shown in the upper panels of Figure 2b–e (D-isomer and L-isomer spectra are shown in red and blue, respectively). A strong excimer CPL band was mainly observed for **Aib2–Aib5**, whereas no or very weak monomer CPL signals were observed. In **Aib2–Aib5**, as in 1–3 (see reference [12]), the excimer CPL was (+)-CPL in the D-isomer and (–)-CPL in the L-isomer. These CPL spectra were comparable but mirror images of one another. These excimer CPL signals originated from the multiple pyrene units located at distant locations within the molecule of the peptide backbone with the same chirality. The absolute anisotropy factor values for the excimer CPL,  $g_{\text{CPL}}$ , were  $+6.7 \times 10^{-3}$  (D-isomer) and  $-7.0 \times 10^{-3}$  (L-isomer) for **Aib2**,  $+4.6 \times 10^{-3}$  (D-isomer) and  $-4.0 \times 10^{-3}$  (L-isomer) for **Aib3**,  $+4.7 \times 10^{-3}$  (D-isomer) and  $-4.4 \times 10^{-3}$  (L-isomer) for **Aib4**, and  $+5.7 \times 10^{-3}$  (D-isomer) and  $-5.9 \times 10^{-3}$  (L-isomer) for **Aib5**. The obtained CPL

and PL properties are summarized in Table 1 together with other key data. The CPL data of **Aib1–5** and **1–3** in ethanol solution are included in the Supporting Information (Figures S21a–e and S22a–c). As shown, in ethanol, clear excimer CPL was observed in the cases of **Aib1–Aib5**. However, only **1** exhibited a clear excimer CPL, with no clear excimer CPL being observed for **2** and **3**. In the cases of **Aib1–Aib5**, no aggregates were observed when dissolved in ethanol. However, in the case of **3**, small aggregates were detected. The CPL data obtained in ethanol solution are summarized in the Supporting Information (Table S1).

**Table 1.** CPL, PL, circular dichroism (CD), and UV–Vis properties of peptide-pyrene luminophores in CHCl<sub>3</sub>.

Name	Monomer PL (nm)	Excimer PL (nm)	$\Phi_F$	gCPL ( $\times 10^{-3}$ )	$\lambda_{CD}$ (nm)	gCD ( $\times 10^{-4}$ )	Note
D-Aib1	379	ND		ND		+1.5	
L-Aib1	379	ND	0.11	ND	345	−1.7	
D-Aib2	395.5	473.5		+6.7		−1.1	
L-Aib2	395.5	474.5	0.12	−7.0	347.5	+1.3	
D-Aib3	395.5	460.5		+4.6		−2.3	
L-Aib3	395.5	453.5	0.12	−4.0	346.5	+2.4	
D-Aib4	395.5	449		+4.7		−1.6	
L-Aib4	395.5	448	0.14	−4.4	346	+1.6	
D-Aib5	395.5	451.5		+5.7		−7.3	
L-Aib5	395.5	451.5	0.17	−5.9	346	+7.7	
D-Gly1 [13]	398	481.5					
L-Gly1 [13]	398	481.5	0.12	$\pm 2.0$	346	$\pm 0.90$	
D-Gly3	ND	ND		ND		+20	Aggregated
L-Gly3	ND	ND	0.08	ND	361.5	−18	Aggregated
D-Gly5	ND	ND		ND		+5.2	Aggregated
L-Gly5	ND	ND	0.11	ND	361	−7.8	Aggregated
D-1 [12]	395.5	463		+11			
L-1 [12]	379	455	0.10	−8.6	349	$\mp 0.91$	
D-2 [12]	396	454		+8.5			
L-2 [12]	396	460	0.12	−8.4	351	$\mp 1.2$	
D-3 [12]	396	454		+2.7			
L-3 [12]	396	456	0.15	−3.3	351	$\mp 1.1$	

To examine the ground-state chiralities of **Aib1–Aib5**, we compared their CD and UV–Vis absorption spectra in the CHCl<sub>3</sub> solution (Figure 3a–e). The  $\lambda_{CD}$  values of **D-Aib1–D-Aib5** were as follows: 345, 347.5, 346.5, 346, and 346 nm, respectively, while the gCD values of ground-state chirality [15] were  $+1.5 \times 10^{-4}$  (D-isomer) and  $-1.7 \times 10^{-4}$  (L-isomer) for **Aib1**,  $-1.1 \times 10^{-4}$  (D-isomer) and  $+1.3 \times 10^{-4}$  (L-isomer) for **Aib2**,  $-2.3 \times 10^{-4}$  (D-isomer) and  $+2.4 \times 10^{-4}$  (L-isomer) for **Aib3**,  $-1.6 \times 10^{-4}$  (D-isomer) and  $+1.6 \times 10^{-4}$  (L-isomer) for **Aib4**, and  $-7.3 \times 10^{-4}$  (D-isomer) and  $+7.7 \times 10^{-4}$  (L-isomer) for **Aib5**. Interestingly, **D-Aib1** exhibited a positive (+) first Cotton band, while **D-Aib2–D-Aib5** gave negative (-) Cotton bands. In addition, monomer CPL was observed for **Aib1**, but clear excimer CPL was observed for **Aib2–Aib5**. Furthermore, the sign of  $\lambda_{CD}$  was inverted between **Aib1** and **Aib2–Aib5**. The difference in the Cotton CD band at approximately 350 nm derived from the pyrene unit suggests the occurrence of excimer CPL. The obtained CD and UV–Vis properties are summarized in Table 1 together with other key data. The CD data of **Aib1–5** and **1–3** in ethanol are provided in the Supporting Information (Figures S23a–e and S24a–c). The CD data obtained in ethanol solution are summarized in the Supporting Information (Table S1).

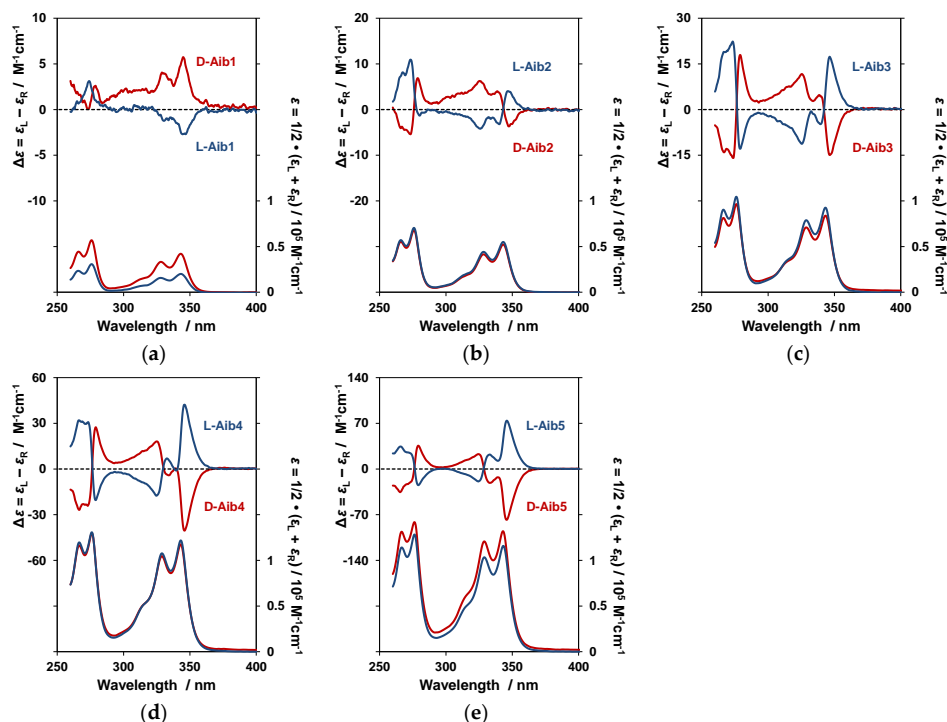


**Figure 3.** CD (upper panel) and UV-Vis (lower panel) spectra of (a) **D-Aib1/L-Aib1**; (b) **D-Aib2/L-Aib2**; (c) **D-Aib3/L-Aib3**; (d) **D-Aib4/L-Aib4**; and (e) **D-Aib5/L-Aib5** in  $\text{CHCl}_3$  ( $1.0 \times 10^{-4}$  M). D-isomer and L-isomer spectra are shown by red and blue lines, respectively. Path length = 1 mm.

### 3.2. Measurement of Gly1, Gly3, and Gly5 Circularly Polarized Luminescence (CPL) and Photoluminescence (PL) Spectra and Circular Dichroism (CD) and UV-Vis Absorption Spectra in $\text{CHCl}_3$ Solution

The CPL spectra of the Gly units exhibiting less steric hindrance (i.e., **Gly1**, **Gly3**, and **Gly5**) in the  $\text{CHCl}_3$  solution are shown in Figure 4a–c. In the case of **Gly1**, monomer CPL and excimer CPL from the pyrene unit were both observed. However, no CPL characteristics were observed for **Gly3** and **Gly5**, where the formation of aggregates was observed when mixed with  $\text{CHCl}_3$ . Indeed, the  $\text{CHCl}_3$  solution was a cloudy suspension that did not transmit sufficient light. It is possible that aggregate formation in **Gly1**, **Gly3**, and **Gly5** results in their solution concentrations being too low to allow sufficient CPL detection. The obtained CPL and PL properties are summarized in Table 1 together with other key data. The CPL data of **Gly1**, **Gly3**, and **Gly5** in ethanol are provided in the Supporting Information (Figure S25a–c). It was found that aggregate formation also took place in the cases of **Gly3** and **Gly5** in the ethanol solution. The CPL data obtained in ethanol solution are summarized in the Supporting Information (Table S1).

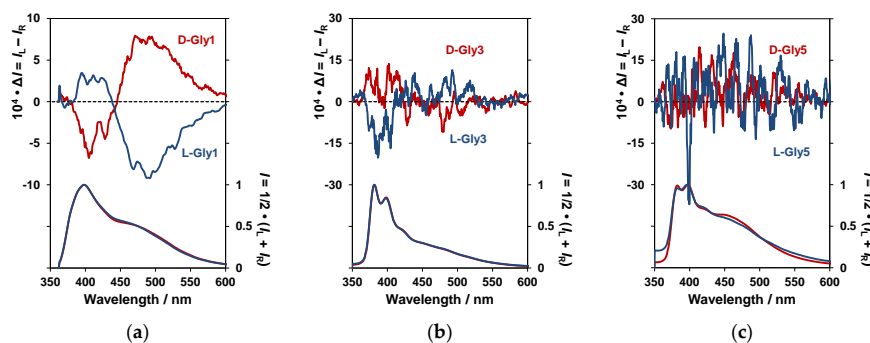


**Figure 4.** CPL (upper panel) and PL (lower panel) spectra of (a) **D-Gly1/L-Gly1** [13]; (b) **D-Gly3/L-Gly3**; (c) **D-Gly5/L-Gly5** in  $\text{CHCl}_3$  ( $1.0 \times 10^{-4}$  M). D-isomer and L-isomer spectra are shown in red and blue, respectively. Path length = 1 mm.

To examine the ground-state chiralities of **Gly1**, **Gly3**, and **Gly5**, we compared their CD and UV–Vis absorption spectra in the  $\text{CHCl}_3$  solution (Figure 5a–c). In the case of **Gly1**, it was observed in the UV–Vis spectra as well as in those of **Aib1** and **1**, but was hardly detected in the cases of **Gly3** and **Gly5**. It was therefore considered that their CPL spectra exhibit the same phenomenon. In the Gly peptide, the degree of freedom of the peptide increased when the number of Gly units and pyrene units was increased, as the likelihood of aggregate formation between the pyrene units increased. The obtained CD and UV–Vis properties are summarized in Table 1 together with other key data. The CD data of **Gly1**, **Gly3**, and **Gly5** in the ethanol solution are provided in the Supporting Information (Figure S26a–c).

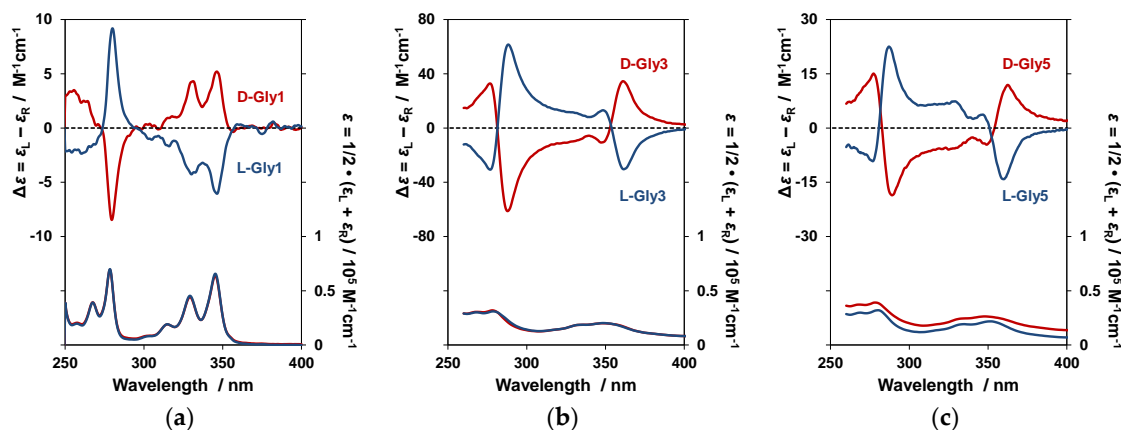


**Figure 5.** CD (upper panel) and UV–Vis (lower panel) spectra of (a) **D-Gly1/L-Gly1** [13]; (b) **D-Gly3/L-Gly3**; (c) **D-Gly5/L-Gly5** in  $\text{CHCl}_3$  ( $1.0 \times 10^{-4}$  M). D-isomer and L-isomer spectra are shown in red and blue, respectively. Path length = 1 mm.

#### 4. Conclusions

We developed peptide-pyrene organic luminophores containing the Aib unit. The Aib peptide exhibited excimer CPL in both chloroform and ethanol solutions upon increasing the number of pyrene units. In the ethanol solution, the compounds bearing no Aib unit exhibited trace aggregate formation when four pyrene units were introduced into the peptide. However, it was observed that upon introduction of the Aib unit, no aggregate formation occurred, even when the number of pyrenes was increased to six. Furthermore, when the Gly unit was introduced, the aggregate formation was observed in both chloroform and ethanol solutions when four pyrene units were introduced. Therefore, it was found that there is a high possibility that aggregates will be formed simply by increasing the distance between the pyrene units. In contrast to the Gly peptide, the steric hindrance of the Aib unit inhibits the formation of aggregates, and the number of Gly units can also be adjusted to regulate aggregate formation. We believe that our results may be of assistance in designing future materials using peptide-pyrene organic luminophores.

**Supplementary Materials:** The following are available online at <http://www.mdpi.com/2227-9717/8/12/1550/s1>, Figure S1–S10: MALDI-TOF mass spectrum of Aib peptides. Figure S11–S20: RP-HPLC chart of Aib peptides. Figure S21: CPL and PL spectra of **Aib1–Aib5** in ethanol. Figure S22: CPL and PL spectra of **1–3** in ethanol. Figure S23: CD and UV–Vis spectra of **Aib1–5** in ethanol. Figure S24: CD and UV–Vis spectra of **1–3** in ethanol. Figure S25: CPL and PL spectra of **Gly1**, **Gly3**, and **Gly5** in ethanol. Figure S26: CD and UV–Vis spectra of **Gly1**, **Gly3**, and **Gly5** in ethanol.

**Author Contributions:** Conceptualization, Y.I. and M.K.; methodology, Y.I. and M.K.; software, Y.I.; validation, Y.M. (Yuki Mimura) and Y.M. (Yuki Motomura); formal analysis, Y.M. (Yuki Mimura) and Y.M. (Yuki Motomura); investigation, Y.M. (Yuki Mimura) and Y.M. (Yuki Motomura); resources, Y.I. and M.K.; data curation, Y.I. and M.K.; writing—original draft preparation, Y.M. (Yuki Mimura); writing—review and editing, Y.I. and M.K.; visualization, Y.I. and Y.M. (Yuki Mimura); supervision, Y.I.; project administration, Y.I. and M.K.; funding acquisition, Y.I. All authors have read and agreed to the published version of the manuscript.

**Funding:** This study was supported by Grants-in-Aid for Scientific Research (18K05094, 19H02712, 19H04600, and 20H04678) from MEXT/Japan Society for the Promotion of Science; the Research Foundation for KDDI (2019-9); the Electrotechnology of Chubu (R-30506); Futaba (2019-6); Murata Science Foundation (H31-007); the Nippon Sheet Glass Foundation for Materials Science and Engineering (H30-4); the Yashima Environment Technology Foundation (2019-No9). This work was also supported by JST, CREST (JPMJCR2001), Japan.

**Conflicts of Interest:** The authors declare no conflict of interest. The funding sponsors had no role in the design of the study; in the collection, analyses, or interpretation of data; in the writing of the manuscript; nor in the decision to publish the results.

## References

1. Field, J.E.; Muller, G.; Riehl, J.P.; Venkataraman, D. Circularly Polarized Luminescence from Bridged Triarylamine Helicenes. *J. Am. Chem. Soc.* **2003**, *125*, 11808–11809. [[CrossRef](#)] [[PubMed](#)]
2. Maeda, H.; Bando, Y. Recent progress in research on stimuli-responsive circularly polarized luminescence based on  $\pi$ -conjugated molecules. *Pure Appl. Chem.* **2013**, *85*, 1967–1978. [[CrossRef](#)]
3. Sanchez-Carnerero, E.M.; Agarrabeitia, A.R.; Moreno, F.; Maroto, B.L.; Muller, G.; Ortiz, M.J.; Moya, S. Circularly Polarized Luminescence from Simple Organic Molecules. *Chem. Eur. J.* **2015**, *21*, 13488–13500. [[CrossRef](#)] [[PubMed](#)]
4. Kumar, J.; Nakashima, T.; Kawai, T. Circularly Polarized Luminescence in Chiral Molecules and Supramolecular Assemblies. *J. Phys. Chem. Lett.* **2015**, *6*, 3445–3452. [[CrossRef](#)] [[PubMed](#)]
5. Longhi, G.; Castiglioni, E.; Kosyoubu, J.; Mazzeo, G.; Sergio, A. Circularly Polarized Luminescence: A Review of Experimental and Theoretical Aspects. *Chirality* **2016**, *28*, 696–707. [[CrossRef](#)] [[PubMed](#)]
6. Sun, Z.; Suenaga, T.; Sarkar, P.; Sato, S.; Kotani, M.; Isobe, H. Stereoisomerism, crystal structures, and dynamics of belt-shaped cyclonaphthylenes. *Proc. Natl. Acad. Sci. USA* **2016**, *113*, 8109–8114. [[CrossRef](#)] [[PubMed](#)]
7. Tanaka, H.; Inoue, Y.; Mori, T. Circularly Polarized Luminescence and Circular Dichroisms in Small Organic Molecules: Correlation between Excitation and Emission Dissymmetry Factors. *ChemPhotoChem* **2018**, *2*, 386–402. [[CrossRef](#)]
8. Pop, F.; Zigon, N.; Avarvari, N. Main-Group-Based Electro- and Photoactive Chiral Materials. *Chem. Rev.* **2019**, *119*, 8435–8478. [[CrossRef](#)]
9. Ma, J.-L.; Peng, Q.; Zhao, C.-H. Circularly Polarized Luminescence Switching in Small Organic Molecules. *Chem. Eur. J.* **2019**, *25*, 15441–15454. [[CrossRef](#)] [[PubMed](#)]
10. Ohishi, Y.; Inouye, M. Circularly polarized luminescence from pyrene excimers. *Tetrahedron Lett.* **2019**, *60*, 151232. [[CrossRef](#)]
11. Gao, J.; Zhang, W.Y.; Wu, Z.G.; Zheng, Y.X.; Fu, D.W. Enantiomorphic Perovskite Ferroelectrics with Circularly Polarized Luminescence. *J. Am. Chem. Soc.* **2020**, *142*, 4756–4761. [[CrossRef](#)] [[PubMed](#)]
12. Nishikawa, T.; Tajima, N.; Kitamatsu, M.; Fujiki, M.; Imai, Y. Circularly polarised luminescence and circular dichroism of L- and D-oligopeptides with multiple pyrenes. *Org. Biomol. Chem.* **2015**, *13*, 11426–11431. [[CrossRef](#)] [[PubMed](#)]
13. Nishikawa, T.; Kitamura, S.; Kitamatsu, M.; Fujiki, M.; Imai, Y. Peptide Magic: Interdistance-Sensitive Sign Inversion of Excimer Circularly Polarized Luminescence in Bipyrenyl Oligopeptides. *ChemistrySelect* **2016**, *4*, 831–835. [[CrossRef](#)]
14. Yuan, W.Z.; Lu, P.; Chen, S.; Lam, J.W.Y.; Wang, Z.; Liu, Y.; Kwok, H.S.; Ma, Y.; Tang, B.Z. Changing the Behavior of Chromophores from Aggregation-Caused Quenching to Aggregation-Induced Emission: Development of Highly Efficient Light Emitters in the Solid State. *Adv. Mater.* **2010**, *22*, 2159–2163. [[CrossRef](#)] [[PubMed](#)]
15. The absolute CD magnitude using the dimensionless Kuhn's anisotropy factor in the ground state is defined as  $g_{CD} = \Delta\epsilon/\epsilon$ .

**Publisher's Note:** MDPI stays neutral with regard to jurisdictional claims in published maps and institutional affiliations.



© 2020 by the authors. Licensee MDPI, Basel, Switzerland. This article is an open access article distributed under the terms and conditions of the Creative Commons Attribution (CC BY) license (<http://creativecommons.org/licenses/by/4.0/>).